

Robust Volt/VAr Control With Photovoltaics

Rabih A. Jabr , Fellow, IEEE

Abstract—The new IEEE 1547-2018 standard includes dynamic Volt/VAr control for photovoltaic (PV) smart inverters. While recent research has addressed the problem of optimal inverter dispatch, the interaction between inverters and the classical Volt/VAr control (VVC) regulation system needs further study. This paper proposes an approach that builds on the classical VVC solution with PVs, by computing for each inverter a rule that modulates the smart inverter reactive power in function of its real power. Two approaches are presented for computing the inverter's reactive power equation slope: the first approach is based on the robust minimization of the absolute voltage magnitude deviation via a linear program, whereas the second approach yields closed-form solutions inspired from distributionally robust chance constraints. Numerical results are presented on weakly meshed distribution networks having up to 3146 nodes; they demonstrate that the voltage violations due to intermittent real power variations are significantly reduced by the decision rules as compared to maintaining the last computed VVC set-points, even when the inverters operate at constant power factor or with default Volt/VAr settings proposed in the literature; additionally, the reactive power decision rules maintain a network loss level that is close to the average from a centralized solution.

Index Terms—Decentralized control, distributed power generation, load flow control, optimization methods, reactive power control, uncertainty, voltage control.

I. INTRODUCTION

THE voltages in distribution networks are classically regulated using switched capacitors and load tap changers (LTCs) installed on substation transformers and step voltage regulators [1]. The increased distributed generation from photovoltaics results in voltage fluctuations associated with the real power intermittency [2]; the regulation of voltages using the legacy switched-type devices would require their frequent operation, which may translate into more repeated maintenance and eventually reduced life cycle. The national IEEE 1547-2003 standard did not require dynamic voltage support on distributed energy resources such as photovoltaics; however the new IEEE 1547-2018 standard stipulates specific voltage support requirements, for instance by means of the smart inverter reactive power control [3]. The inverter reactive power dispatch alleviates the stress of frequent operation on legacy voltage controllers and allows them to run at a slower time scale; however, the interaction between the inverters and the classical voltage regulation

devices is a problem that requires further study [3]. Recent research has addressed the use of distributed energy resources as a source/sink of reactive power that has to be coordinated with the selection of set-points for the legacy voltage regulation devices [4]; given the slower time scale of switched-type devices, this paper studies the reactive power dispatch of smart inverters in the time interval before the VVC set-points are recomputed and implemented in the field. The proposed dispatch is based on optimized local decision rules that are communicated to the smart inverters at the same time as the VVC set-points, thus reducing the computational and communication overhead.

The solution to the problem of coordinating optimal inverter dispatch with other voltage regulation devices can be classified into three main categories based on communication requirements [5]: centralized, distributed, and decentralized. The centralized solution has its computational engine similar to that of transmission network optimal power flow methods [6]–[8]; the centralized solution can also account for temporal constraints over several time periods, and the different time scales for controlling switched-type devices and photovoltaic (PV) inverters [9]. The distributed methods essentially solve the same problem as in the centralized method, but the computations are distributed amongst the different inverters [10]–[12]; the inverters solve the sub-problems in parallel and the neighboring ones exchange information throughout the iterative process. The convergence of distributed methods is however highly dependent on the convexity of the network model. The decentralized methods compute the reactive power contributions using a control law that takes local measurements as inputs. The parameters of the control law can either be communicated to the smart inverters at regular time intervals, or they could be implemented at the time of installation (purely local control) [13], [14]. An interesting purely local control scheme is the incremental control based on voltage measurements [15], [16], but it tends to stabilize the voltage in a specified range only at the inverter nodes.

The control law inherent in a decentralized implementation can have its parameters optimized via methods that consider the uncertainty characterization of photovoltaic generation. The most commonly employed decision rule is an affine function of the uncertain parameters, and whose coefficients can be computed using chance-constrained optimization [17]. Chance-constrained optimization requires specifying probability density functions for the uncertain parameters, but these functions cannot be known with certainty. In the distribution network power flow optimization context, the characterization of uncertainty with partial information has been addressed via distributionally robust chance-constrained programming [18] and robust optimization [19]–[22]; these approaches broadly differ by ei-

Manuscript received July 27, 2018; revised November 6, 2018; accepted December 31, 2018. Date of publication January 3, 2019; date of current version April 17, 2019. This work was supported in part by the National Council for Scientific Research in Lebanon and in part by the American University of Beirut. Paper no. TPWRS-01157-2018.

The author is with the Department of Electrical and Computer Engineering, American University of Beirut, Beirut 1107 2020, Lebanon (e-mail: rabih.jabr@aub.edu.lb).

Digital Object Identifier 10.1109/TPWRS.2018.2890767

ther allowing the parameters of the probability distribution to vary in an uncertainty set as in distributionally robust chance-constrained optimization, or by having the uncertain parameters themselves vary in the uncertainty set as in robust optimization. However, the distributionally robust and other robust-type formulations [18]–[22] require a linear network model for the underlying theory to hold. Even with a linear power flow approximation, the distributionally robust chance-constrained formulation is of higher order, typically a second-order conic or a semidefinite program [23], [24].

While the accuracy of the linearized power flow model tends to be sufficient for transmission network optimal power flow [23], [24] and distribution network reactive power dispatch [17]–[22], this does not hold for VVC. Classical VVC operates on switched-type devices, whose discrete set-point changes cannot be accurately captured via a linear network model. To address this shortcoming, this paper proposes a decentralized approach for inverter dispatch that builds on a centralized VVC solution employing the full AC network model; for a given load and PV generation forecast, the VVC solution optimizes the discrete settings of LTCs and switched capacitors, together with the reactive power from smart inverters. To minimize wear-and-tear on switched type devices, the VVC solution is practically recomputed at a fixed time-step of around 15 minutes and executed on the network either in closed-loop mode or in advisory mode [25]; this practice was sufficient in distribution networks having small-capacity distributed generation. With the increased capacity of distributed generation, the intermittency of real power injections can cause unacceptable voltage excursions if the legacy controllers are maintained to operate at their original set-points. To minimize such voltage fluctuations, this paper proposes using an affine control law for adjusting the inverter reactive power in function of the real power variation. For an inverter at node k , the affine Watt/VAr control law is of the form $Q_k = \hat{Q}_k + \alpha_k \Delta P_k$, with \hat{Q}_k computed from the classical VVC coordination problem; the coefficient α_k is then optimally computed to minimize the deviation in network voltages due to active power fluctuation (ΔP_k). Two practical approaches are investigated for computing the reactive power equation slope: one based on robust optimization leading to a linear program, and the other on a distributionally robust chance-constrained linear program resulting in a closed-form solution. A robust optimization approach for decentralized inverter dispatch has been previously proposed in [20], however [20] does not present any type of closed-form solutions. The linear decision rules herein operate on a network whose control set points have been obtained via VVC, and the model employed in computing the slope of the inverter is based on a linearization around the current VVC operating point; it is therefore bound to be more accurate than the network model used in [20], which is effectively a linearization around the no-load operating point.

The rest of this paper is organized as follows. Section II reviews the VVC solution with inverter reactive dispatch, and Section III presents the two approaches for computing the slope of the inverter's reactive power decision rule. Numerical results are presented in Section IV on distribution networks having up to 3146 nodes; with the switched-type controllers operating at

their last setting, the proposed decision rules are contrasted with (i) maintaining the reactive inverter power at the last computed VVC set-point, (ii) operating each inverter at constant power factor, (iii) operating each inverter based on the default Volt/VAr settings as proposed by the IEEE Voltage Regulation Subgroup [14], and (iv) dispatching the inverters according to centralized optimization. The paper is concluded in Section V.

II. CENTRALIZED VOLT/VAr CONTROL

Centralized VVC became popular in the 1980s and its adoption increased with the development of low-cost radio-based communication links to the voltage and VAr controllers [25]. Nowadays VVC in SCADA-based distribution management systems is commonly based on network applications such as topology processing, distribution state estimation, and distribution power flow. The distribution state estimator provides estimates of the load consumption and distributed generation power levels [26], which together with the network's topology and parameters are required as inputs to centralized VVC. The primary objective of VVC is to remove voltage violations, with a secondary objective such as power loss minimization [4], [25], [27], [28]. Mathematically, it can be formulated as an optimization problem whose objective is to minimize the network losses while keeping voltage magnitudes within their prescribed limits [4]. The typical VVC implementation that is adopted by the industry is power-flow based, with the optimization guided by multistep discrete programming. At the current operating point, the initial objective function (IOF) is computed as in (1):

$$f = P_{Loss} + C_V \sum_{i=1}^n \max(0, |V_i| - |V_i|^{\max}) + C_V \sum_{i=1}^n \max(0, |V_i|^{\min} - |V_i|) \quad (1)$$

where P_{Loss} is the total power loss, $|V_i|$ is the voltage magnitude at node i , n is the number of nodes, and C_V is the penalty term for voltage violations. The discrete-coordinate descent optimization engine iteratively searches for control actions that may improve the objective function value, and uses power flow to test their efficacy. When the search terminates with an optimal objective value strictly less than the IOF, the corresponding optimal control actions (LTC tap positions, capacitor bank statuses, and distributed generation reactive power settings) are prepared for implementation by SCADA [25].

The most time-consuming part of VVC is the power flow solution, as a typical distribution network can have few thousand nodes; the power flow is carried out using backward/forward sweep for radial networks and the nodal admittance matrix methods for weakly meshed ones. The fact that the network topology remains unchanged during the VVC iterations helps to speed up the search, as the matrix ordering and factorization are carried out once at the beginning of the iterations; any subsequent changes in the LTC tap and capacitor settings are then accounted for via the compensation technique without resort to re-factorization [4], [25], [27]. Ref. [4] presented an approach to further improve the execution time of VVC by reducing the

number of power flow solutions; this was accomplished by using sensitivity analysis to directly discard the search directions that cannot lead to improvement in the VVC objective function value.

The VVC solution is optimal for the snapshot of the system given by the distribution state estimator; its implementation on the network devices (e.g. by directly changing the LTC tap positions and capacitor switch statuses) is carried out in two possible modes: closed-loop mode that executes control actions automatically, or advisory mode that requires the operator's approval before implementation [25]. In any case, the periodicity of the VVC solution is typically around 15 minutes, during which the variations of the PV real power generation may give rise to significant voltage violations. The rule-based dispatch proposed in Section III aims to reduce possible voltage fluctuations, by modulating the inverter's reactive power in function of its real power. The envisaged solution is independent of the specific centralized VVC solver; it simply requires communicating to the smart inverter the slope of the reactive power linear decision rule in addition to the nominal set-points computed by VVC. A required assumption in some previous studies of decentralized inverter dispatch is that communication with the inverters can be executed as part of the VVC infrastructure [13], [21], [22]. In the event that the PV real power does not vary from the value used in the last VVC execution, the rule-based dispatch will maintain the inverter's reactive at its previously computed value.

III. DECENTRALIZED RULE-BASED INVERTER DISPATCH

The decentralized inverter reactive power dispatch is based on the following linear decision (Watt/VAR) rule [17], [20]–[22]:

$$Q_k = \hat{Q}_k + \Delta Q_k = \hat{Q}_k + \alpha_k \Delta P_k \quad (2)$$

where \hat{Q}_k is the inverter reactive power computed from centralized VVC and coordinated with the settings of the LTC taps and capacitor banks (Section II), and α_k is the slope of the linear decision rule; ΔP_k is an uncertain parameter representing the variation of the PV real power generation around its forecasted value \hat{P}_k (\hat{P}_k is employed in the VVC solution):

$$\Delta P_k \in [\Delta P_k^{\min}, \Delta P_k^{\max}] \quad (3)$$

The minimum and maximum limits of the uncertain parameter in (3) are such that:

$$\Delta P_k^{\min} \leq 0 \leq \Delta P_k^{\max} \quad (4)$$

The inverter's apparent power capacity S_k^{\max} is typically set to 10% above the real power rating of the connected PV system [13], [14]. If the linear decision rule (2) gives rise to an apparent power value that is in excess of the inverter's rating, the reactive power from (2) is projected back to the boundary of the inverter's capability diagram [13]:

$$Q_k = \text{Constr} \left(\hat{Q}_k + \alpha_k \Delta P_k, \sqrt{(S_k^{\max})^2 - (\hat{P}_k + \Delta P_k)^2} \right) \quad (5)$$

where

$$\text{Constr}(x, x^{\max}) = \begin{cases} x, & |x| \leq x^{\max} \\ (x/|x|) x^{\max}, & \text{otherwise} \end{cases} \quad (6)$$

The aim of this section is to compute the slope α_k of the decision rule for each of the smart inverters. Consider a distribution network having n nodes, and without loss of generality, let node 1 represent the slack node (substation connection), nodes $2, \dots, m$ represent nodes having photovoltaic connections, and nodes $m+1, \dots, n$ represent load nodes. The network Jacobian matrix is formed by considering nodes $2, \dots, n$ as PQ-type nodes, and uses the network nodal admittance matrix that accounts for the LTC off-nominal tap positions and switched capacitor settings from VVC:

$$\begin{bmatrix} \Delta P_{(n-1) \times 1} \\ \Delta Q_{(n-1) \times 1} \end{bmatrix} = \begin{bmatrix} J^{P\delta} & J^{P|V|} \\ J^{Q\delta} & J^{Q|V|} \end{bmatrix} \begin{bmatrix} \Delta \delta_{(n-1) \times 1} \\ \Delta |V|_{(n-1) \times 1} \end{bmatrix} \quad (7)$$

where each of the sub-matrices in the Jacobian matrix (7) is of size $(n-1) \times (n-1)$, δ is the vector nodal angles, and $|V|$ is the vector of nodal voltage magnitudes at nodes $2, \dots, n$. The elements of the Jacobian matrix are given by:

$$J_{ij}^{P\delta} = \frac{\partial P_i}{\partial \delta_j} \Big|_{VVC}, \quad J_{ij}^{P|V|} = \frac{\partial P_i}{\partial |V|_j} \Big|_{VVC} \quad (8)$$

$$J_{ij}^{Q\delta} = \frac{\partial Q_i}{\partial \delta_j} \Big|_{VVC}, \quad J_{ij}^{Q|V|} = \frac{\partial Q_i}{\partial |V|_j} \Big|_{VVC} \quad (9)$$

The sensitivity equation (7) can be inverted into:

$$\begin{bmatrix} \Delta \delta_{(n-1) \times 1} \\ \Delta |V|_{(n-1) \times 1} \end{bmatrix} = \begin{bmatrix} K^{\delta P} & K^{\delta Q} \\ K^{|V|P} & K^{|V|Q} \end{bmatrix} \begin{bmatrix} \Delta P_{(n-1) \times 1} \\ \Delta Q_{(n-1) \times 1} \end{bmatrix} \quad (10)$$

Therefore, the voltage magnitude deviation at node j ($j = 2, \dots, n$) due to the fluctuation of the PV real power at nodes $2, \dots, m$ can be approximated by:

$$\begin{aligned} \Delta |V|_j &= \sum_{k=2}^m \left(K_{jk}^{|V|P} \Delta P_k + K_{jk}^{|V|Q} \Delta Q_k \right) \\ &= \sum_{k=2}^m \left(K_{jk}^{|V|P} + K_{jk}^{|V|Q} \alpha_k \right) \Delta P_k \end{aligned} \quad (11)$$

Eq. (11) makes use of the elements in the first $(m-1)$ columns from each of the two $(2n-2) \times (n-1)$ blocks in the inverse Jacobian matrix (10); these values can be computed without requiring a complete inversion of the Jacobian matrix, rather the sparse Jacobian matrix is ordered and LU factorized, and the desired columns are calculated via forward/backward substitution.

Two approaches are presented below for computing α_k ($k = 2, \dots, m$), starting from the voltage magnitude sensitivity equation (11). The first approach in subsection III-A is based on affinely adjustable robust optimization theory [29], and the second approach in subsection III-B is inspired from the distributionally robust chance-constrained linear programming formulation [30].

A. Robust Optimization Solution

Consider the problem of minimizing the sum of absolute voltage magnitude deviations at all nodes except the slack:

$$\min \sum_{j=2}^n \left| \Delta |V|_j \right| \quad (12)$$

Using (11), (12) reduces to:

$$\min \sum_{j=2}^n \left| \sum_{k=2}^m \left(K_{jk}^{|V|P} + K_{jk}^{|V|Q} \alpha_k \right) \Delta P_k \right| \quad (13)$$

Problem (13) can be written without the absolute value operator by introducing auxiliary variables t_j ($j = 2, \dots, n$):

$$\min \sum_{j=2}^n t_j \quad (14)$$

subject to:

$$t_j \geq \sum_{k=2}^m \left(K_{jk}^{|V|P} + K_{jk}^{|V|Q} \alpha_k \right) \Delta P_k \quad (15)$$

$$t_j \geq \sum_{k=2}^m \left(K_{jk}^{|V|P} + K_{jk}^{|V|Q} \alpha_k \right) (-\Delta P_k) \quad (16)$$

$$j = 2, \dots, n \quad (17)$$

Given that ΔP_k varies in the uncertainty interval (3), the corresponding affinely adjustable robust counterpart (AARC) of (14)–(17) is [29]:

$$\min \sum_{j=2}^n t_j \quad (18)$$

subject to:

$$t_j \geq \sum_{k=2}^m \left[\theta'_{jk} \Delta P_k^{\max} + \theta''_{jk} \Delta P_k^{\min} \right] \quad (19)$$

$$t_j \geq \sum_{k=2}^m \left[\theta'_{jk} (-\Delta P_k^{\min}) + \theta''_{jk} (-\Delta P_k^{\max}) \right] \quad (20)$$

$$j = 2, \dots, n \quad (21)$$

$$\theta'_{jk} \geq 0, \quad \theta'_{jk} \geq K_{jk}^{|V|P} + K_{jk}^{|V|Q} \alpha_k \quad (22)$$

$$\theta''_{jk} \leq 0, \quad \theta''_{jk} \leq K_{jk}^{|V|P} + K_{jk}^{|V|Q} \alpha_k \quad (23)$$

$$j = 2, \dots, n, \quad k = 2, \dots, m \quad (24)$$

The AARC (18)–(24) is a linear program, whose solution gives the values of the inverter's reactive power equation slope α_k ($k = 2, \dots, m$).

B. Closed-Form Solution

Consider that ΔP_k is a random variable with zero mean and known to belong with probability one to the bounded interval (3); this is reasonable given that the interval limits can be chosen to conform to the real PV inverter power. The interval width of

(3) is:

$$L_k = \Delta P_k^{\max} - \Delta P_k^{\min} \quad (25)$$

Define $L = [L_2, \dots, L_m]$ as the vector of widths of ΔP_k ($k = 2, \dots, m$). With ΔP_k varying over independent bounded intervals ($\Delta P \sim L$), the distributionally robust chance constraint for any $\epsilon \in (0, 1)$ [30]:

$$\inf_{\Delta P \sim L} \Pr \left\{ \Delta |V|_j \leq \Delta |V|_j^{\max} \right\} \geq 1 - \epsilon \quad (26)$$

holds if:

$$\sqrt{\frac{1}{2} \ln \frac{1}{\epsilon}} \sqrt{\sum_{k=2}^m \left(\left(K_{jk}^{|V|P} + K_{jk}^{|V|Q} \alpha_k \right) L_k \right)^2} \leq \Delta |V|_j^{\max} \quad (27)$$

Similarly,

$$\inf_{\Delta P \sim L} \Pr \left\{ \Delta |V|_j \geq \Delta |V|_j^{\min} \right\} \geq 1 - \epsilon \quad (28)$$

holds if:

$$\sqrt{\frac{1}{2} \ln \frac{1}{\epsilon}} \sqrt{\sum_{k=2}^m \left(\left(K_{jk}^{|V|P} + K_{jk}^{|V|Q} \alpha_k \right) L_k \right)^2} \leq -\Delta |V|_j^{\min} \quad (29)$$

Now define:

$$\tau_j = \sum_{k=2}^m \left(\left(K_{jk}^{|V|P} + K_{jk}^{|V|Q} \alpha_k \right) L_k \right)^2 \quad (30)$$

$$j = 2, \dots, n \quad (31)$$

then (27) and (29) can be reduced into one constraint for each voltage at node $j = 2, \dots, m$:

$$\sqrt{\frac{1}{2} \ln \frac{1}{\epsilon}} \tau_j \leq \min \left(\Delta |V|_j^{\max}, -\Delta |V|_j^{\min} \right) \quad (32)$$

Note that τ_j in (32) is a function of α_k as dictated by (30). The values of α_k from (32), and even the feasibility of their computation, depends on the choice of ϵ . Alternatively, it is possible to compute α_k by using the surrogate objective for minimizing the sum of τ_j :

$$\min \sum_{j=2}^n \sum_{k=2}^m \left(\left(K_{jk}^{|V|P} + K_{jk}^{|V|Q} \alpha_k \right) L_k \right)^2 \quad (33)$$

By switching the order of summations in (33), it becomes evident that the objective function is separable in α_k :

$$\min \sum_{k=2}^m L_k^2 \sum_{j=2}^n \left(K_{jk}^{|V|P} + K_{jk}^{|V|Q} \alpha_k \right)^2 \quad (34)$$

Therefore each value of α_k can be computed independently by minimizing:

$$f_k = \sum_{j=2}^n \left(K_{jk}^{|V|P} + K_{jk}^{|V|Q} \alpha_k \right)^2 \quad (35)$$

By setting:

$$\frac{df_k}{d\alpha_k} = 2 \sum_{j=2}^n K_{jk}^{|V|Q} \left(K_{jk}^{|V|P} + K_{jk}^{|V|Q} \alpha_k \right) = 0 \quad (36)$$

TABLE I
TEST SYSTEM DATA

Net	n	BR	CAP	LTC	PV nb.	PV %	min %	max %
B_R	161	160	2	6	7	57.47	28.73	86.20
B_M	160	160	2	6	7	57.47	28.73	86.20
1k5	1464	1474	8	8	5	68.51	34.25	99.34
3k	3146	3157	13	15	10	84.10	50.46	117.74

TABLE II
INVERTER REACTIVE POWER EQUATION SLOPE α_k

k	B_R		B_M		1k5		3k	
	RO	CF	RO	CF	RO	CF	RO	CF
2	-0.44	-0.44	-0.44	-0.44	0.00	-0.01	0.01	-0.01
3	-0.38	-0.38	-0.38	-0.38	-0.01	-0.01	0.19	0.19
4	-0.45	-0.53	-0.45	-0.53	0.32	0.32	0.03	0.03
5	-0.53	-0.52	-0.53	-0.52	0.24	0.21	0.26	0.26
6	-0.46	-0.56	-0.53	-0.60	-0.19	-0.07	0.16	0.16
7	-0.53	-0.59	-0.45	-0.47			0.15	0.16
8	-0.34	-0.33	-0.34	-0.33			0.19	0.21
9							-0.06	-0.04
10							-0.11	-0.12
11							0.18	0.18

the closed-form solution for α_k ($k = 2, \dots, n$) is obtained as:

$$\alpha_k = - \frac{\sum_{j=2}^n \left(K_{jk}^{|V|Q} K_{jk}^{|V|P} \right)}{\sum_{j=2}^n \left(K_{jk}^{|V|Q} \right)^2} \quad (37)$$

IV. NUMERICAL RESULTS

The inverter rule-based dispatch was tested on four distribution networks: modified radial (B_R) and meshed (B_M) versions of a realistic Brazilian distribution system [31], in addition to two weakly meshed test networks with 1464 (1k5) and 3146 (3k) nodes; the complete data sets of the test networks can be downloaded from [32]. Table I shows for each network the number of nodes (n), branches (BR), switched capacitors (CAP), load tap changers (LTC), and photovoltaic distributed generators (PV nb.); the last three columns respectively show the penetration of the PV generation as a percentage of total load in the data set (PV %), in addition to the limits of minimum (min %) and maximum (max %) generation attributed to the interval of uncertainty (3). The PV inverters have an apparent power capacity that is 10% above the connected capacity of PV real power [13]. The test cases feature significant PV power integration, with the 3k network allowing reverse power flow into the substation at the maximum PV generation condition.

With the PV penetration at the level specified under PV % (in Table I), centralized VVC [4] was used to compute the settings of switched capacitors, LTC taps, and inverter reactive power generation such that the network power loss is minimized while alleviating all voltage violations; the VVC settings are also available for download from [32]. Using the VVC solution operating point, the slope for each of the inverter reactive power decision rules (2) was then computed via robust optimization (RO) as presented in subsection III-A, and the closed-form (CF) solution in subsection III-B. The slope values are shown in Table II using two digits after the decimal point; interestingly, they reveal close agreement between the RO and CF computation

TABLE III
PERCENTAGE OF NODES WITH VOLTAGE VIOLATIONS

Net	PV at Max			Av. over 500 MCS		
	BC	RO	CF	BC	RO	CF
B_R	10.00	0.00	0.00	4.22	0.01	0.06
B_M	10.06	0.00	0.00	4.17	0.03	0.08
1k5	16.34	0.07	0.07	10.06	0.05	0.05
3k	16.22	0.03	0.03	4.94	0.12	0.09

TABLE IV
MAXIMUM VOLTAGE VIOLATION AT A SINGLE NODE [pu]

Net	PV at Max			Av. over 500 MCS		
	BC	RO	CF	BC	RO	CF
B_R	1.72E-02	0.00E+00	0.00E+00	4.49E-03	2.79E-08	1.33E-06
B_M	1.72E-02	0.00E+00	0.00E+00	4.47E-03	1.84E-07	1.50E-06
1k5	1.54E-01	3.62E-04	2.80E-04	2.04E-02	2.94E-04	2.11E-04
3k	1.18E-01	2.70E-05	2.94E-05	9.05E-03	6.67E-04	4.70E-04

approaches. The fact that both approaches give close answers is an indication that they are based on well-posed mathematical formulations that are consistent.

To test the performance of the linear decision rules in the time interval before the re-implementation of centralized VVC on the network devices, a Monte-Carlo simulation was carried out where the PV real power generation was uniformly sampled from its respective uncertainty interval. For each simulated instance of PV real power generation, the settings of the capacitor switch statuses and LTC tap positions were maintained at the last implemented centralized VVC solution, but the inverter's reactive power took three possible values:

- 1) Base Case (BC): the inverter's reactive power is maintained at the last value from centralized VVC, with real power priority in case the real and reactive power require the inverter to operate beyond its nameplate capacity; i.e. the inverter's reactive power is computed according to (5) with $\alpha_k = 0$.
- 2) Robust Optimization (RO): the inverter's reactive power is updated using (5), with the slope α_k computed by solving the linear program (18)–(24).
- 3) Closed-Form (CF): the inverter's reactive power is updated using (5), with the slope α_k computed using (37).

A power flow solution was then obtained for each of the above inverter reactive power scenarios. Given that the primary aim of VVC is to reduce voltage magnitude violations, Tables III–V present statistics related to the voltage violations with the PV generation operating at its maximum (PV at Max - c.f. the last column in Table I), and with the same statistics averaged over 500 Monte-Carlo simulations (Av. over 500 MCS). Table III shows the percentage of nodes whose voltage magnitudes violate the maximum (1.05 pu) or minimum limit (0.95 pu). It is evident that without modulating the inverter's reactive power using the PV real power variation, the percentage of nodes that exhibit voltage violation reached around 10% (Av. over 500 MCS); this percentage dropped to less than 0.13% with the RO- and CF-based decentralized control. To quantify the magnitude of violation, Tables IV and V respectively show the corresponding maximum voltage violation at a single node and the total voltage violation at all nodes. The effect that the rule-based

TABLE V
TOTAL VOLTAGE VIOLATION AT ALL NODES [pu]

Net	PV at Max			Av. over 500 MCS		
	BC	RO	CF	BC	RO	CF
B_R	2.23E-01	0.00E+00	0.00E+00	5.08E-02	5.58E-08	2.67E-06
B_M	2.23E-01	0.00E+00	0.00E+00	5.07E-02	3.69E-07	3.01E-06
1k5	2.70E+01	3.62E-04	2.81E-04	2.39E+00	3.48E-04	2.59E-04
3k	4.18E+01	2.70E-05	2.94E-05	1.20E+00	3.25E-03	1.79E-03

TABLE VI
PERCENTAGE INCREASE IN POWER LOSS RELATIVE TO
CENTRALIZED INVERTER DISPATCH

Net	PV at Max		Av. over 500 MCS	
	RO	CF	RO	CF
B_R	0.80	0.64	0.39	0.32
B_M	0.80	0.64	0.40	0.33
1k5	4.32	4.36	0.83	0.84
3k	5.43	5.18	0.66	0.65

TABLE VII
AARC LINEAR PROGRAM COMPUTING TIME

Net	B_R	B_M	1k5	3k
time [ms]	15.4	23.6	220	547

reactive power dispatch has on mitigating voltage violations is evident from Tables III–V. For instance, when the PV generation swings to its maximum, the RO- and CF-based modulation result in no voltage violations for the B_R and B_M networks, and in one voltage violation for each of the 1k5 and 3k networks; the corresponding voltage violation value is less than 4×10^{-4} pu.

Loss minimization is a secondary objective for VVC. To quantify the effect of the decentralized decision rules on the power loss, a comparison was carried out with centralized inverter dispatch; care was taken to ensure that the centralized inverter solution is close to the global optimum, by starting from a conic programming solution (that is globally optimal for radial networks) and then using coordinate descent to restore feasibility for meshed networks [4]. Table VI shows the percentage by which the power loss from using RO- and CF-based modulation is greater than the centralized loss solution; for the 500 MCS, the average increase in power loss for the four test networks is around 0.57% for RO and 0.53% for CF. In terms of computing overhead, only the RO method requires solving a linear program to compute the inverter slopes. Table VII shows that the time for solving the AARC linear program using CPLEX [33] is less than 550 ms, with the computations carried out on a MacBook Pro having 2.9 GHz Intel Core i5 processor with a memory of 8 GB 2133 MHz.

A. Comparison With Other Techniques

1) *Constant Power Factor Operation:* The centralized VVC solution (Section II) gives the optimal value of the inverter's reactive power \hat{Q}_k for the corresponding real power \hat{P}_k from distribution state estimation. One simple approach to deal with the variability of the PV real power is to maintain the inverter

TABLE VIII
PERCENTAGE OF NODES WITH VOLTAGE VIOLATIONS—OTHER TECHNIQUES

Net	PV at Max			Av. over 500 MCS		
	CPF	CIF	SCIF	CPF	CIF	SCIF
B_R	10.00	2.50	2.50	4.33	3.86	3.85
B_M	10.06	2.52	0.63	4.30	3.58	3.58
1k5	22.62	14.49	11.48	4.77	3.92	1.15
3k	4.17	14.34	8.84	3.46	9.08	3.84

TABLE IX
MAXIMUM VOLTAGE VIOLATION AT A SINGLE NODE
[pu]—OTHER TECHNIQUES

Net	PV at Max			Av. over 500 MCS		
	CPF	CIF	SCIF	CPF	CIF	SCIF
B_R	2.18E-02	5.96E-04	4.78E-04	5.53E-03	1.94E-03	1.90E-03
B_M	2.18E-02	4.94E-04	3.73E-04	5.51E-03	1.77E-03	1.72E-03
1k5	4.75E-02	3.37E-02	2.32E-02	1.13E-02	9.85E-03	2.91E-03
3k	2.12E-02	4.21E-02	2.94E-02	1.49E-02	2.83E-02	1.33E-02

TABLE X
TOTAL VOLTAGE VIOLATION AT ALL NODES [pu]—OTHER TECHNIQUES

Net	PV at Max			Av. over 500 MCS		
	CPF	CIF	SCIF	CPF	CIF	SCIF
B_R	2.96E-01	1.09E-03	6.93E-04	6.64E-02	7.32E-03	7.20E-03
B_M	2.96E-01	6.84E-04	3.73E-04	6.63E-02	6.42E-03	6.28E-03
1k5	3.04E+00	3.47E+00	1.63E+00	4.25E-01	4.98E-01	1.01E-01
3k	5.73E-01	8.33E+00	4.07E+00	9.19E-01	3.80E+00	5.78E-01

operation at constant power factor:

$$\frac{Q_k}{\hat{Q}_k} = \frac{\hat{P}_k + \Delta P_k}{\hat{P}_k} \quad (38)$$

$$\Rightarrow Q_k = \hat{Q}_k + \frac{\hat{Q}_k}{\hat{P}_k} \Delta P_k \quad (39)$$

Note that computing the reactive power Q_k from (39) is in the form of the linear decision rule (2) with $\alpha_k = \frac{\hat{Q}_k}{\hat{P}_k}$. Eq. (39) can also give rise to an apparent power that exceeds the inverter's nameplate capacity; this is handled as previously done by using (6) to enforce real power priority:

$$Q_k = \text{Constr} \left(\hat{Q}_k + \frac{\hat{Q}_k}{\hat{P}_k} \Delta P_k, \sqrt{(S_k^{\max})^2 - (\hat{P}_k + \Delta P_k)^2} \right) \quad (40)$$

Tables VIII, IX, and X show the effect of constant power factor operation (CPF) on the percentage of nodes with voltage violations, the maximum voltage violation at a node, and the total violation at all nodes; as before, two sets of values are reported corresponding to the PV penetration at its maximum, and the average over 500 MCS. The results show that while in some instances the constant power factor operation does give an improvement in the voltage violation indices as compared to the base case (BC: $\alpha_k = 0$), the use of the proposed RO- and CF-based methods to compute α_k remains significantly superior.

2) *Default Volt/VAr Inverter Settings:* Another comparison is carried out with the default Volt/VAr control settings for PV smart inverters as defined by the IEEE Voltage Regulation Subgroup [14], [34]; the settings are intended to define out of the box local control functions that improve system performance

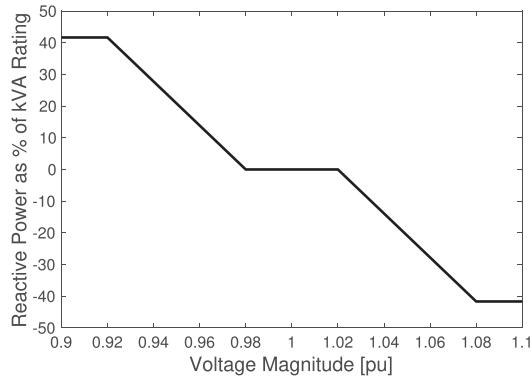


Fig. 1. Common inverter function (CIF).

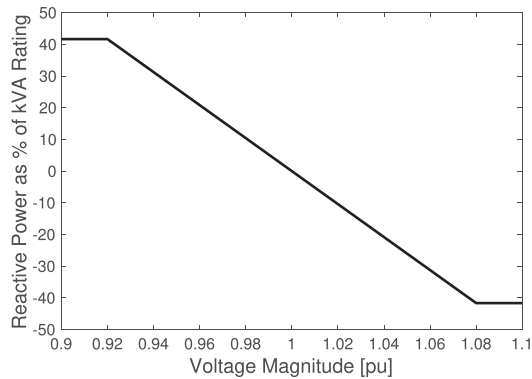


Fig. 2. Simplified common inverter function (SCIF).

without causing any adverse impact. With the inverter apparent power rating sized at 10% above the connected capacity of PV real power, the default setting of maximum reactive power that the inverter can supply or consume is around 42% of the inverter kVA rating ($100 \times \sqrt{1.1^2 - 1^2} / 1.1 \simeq 42\%$). The reactive power contribution in the default Volt/VAr curve is zero when the voltage is in the dead-band ($[0.98 - 1.02]$ pu), and varies linearly when the voltage moves outside the dead-band but remains within $[0.92 - 1.08]$ pu. The default Volt-VAr settings are given in Fig. 1, and the corresponding curve is denoted as the common inverter function (CIF) in Tables VIII–X; a simplified version of the common inverter function (denoted by SCIF) is shown in Fig. 2. The SCIF is similar to the CIF but without a dead-band, to reduce voltage variability. The results in Tables VIII, IX, and X include the statistics of the network performance when using CIF and SCIF. The results show that SCIF is better than CIF in terms of reducing voltage variability due to the absence of the dead-band, and that both the CIF and SCIF tend to improve performance relative to CPF, except for the 3k network with the PV generation at its highest capacity causing reverse power flow. However, given that CIF and SCIF are not optimized for a given system, their performance remains subpar relative to the RO- and CF-based methods.

V. CONCLUSION

This paper presented a rule-based method for decentralized control of photovoltaic inverters; it aims to reduce voltage

violations that may occur due to the fluctuations of PV real power in the time interval between VVC set-point executions in the field. The proposed rule-based method is an add-on to the traditional VVC, and not a replacement; the need for it is motivated by the growing integration of PV capacity in distribution networks, coupled with requirements for voltage support in the new IEEE 1547-2018 standard. The rules for inverter dispatch are communicated to the smart inverters at the time of executing the VVC solution on the network devices. Two methods are proposed for computing the slope of the linear decision rule: a linear program representing an affinely adjustable robust counterpart, and a closed-form solution based on distributionally robust chance-constrained linear programming; the computations in both methods are coordinated with the existing VVC solution. Numerical results are reported on networks with significant PV capacity integration and having up to 3146 nodes; they reveal that both the robust optimization and closed form solutions have very comparable performance, but the simplicity of the closed-form solution makes it more amenable to practical applications. The numerical results also show that the rule-based methods significantly reduce voltage violations as compared to maintaining the previous VVC set-points, even with the options of constant power factor operation and default Volt/VAr settings [14] for smart inverters; they also give rise to a power loss that is on average less than 1% above the centralized inverter dispatch solution.

REFERENCES

- [1] A. Borghetti, "Using mixed integer programming for the volt/var optimization in distribution feeders," *Elect. Power Syst. Res.*, vol. 98, pp. 39–50, 2013.
- [2] P. M. S. Carvalho, P. F. Correia, and L. A. F. M. Ferreira, "Distributed reactive power generation control for voltage rise mitigation in distribution networks," *IEEE Trans. Power Syst.*, vol. 23, no. 2, pp. 766–772, May 2008.
- [3] IEEE PES Industry Technical Support Task Force, "Impact of IEEE 1547 standard on smart inverters," May 2018.
- [4] R. A. Jabr and I. Džafić, "Sensitivity-based discrete coordinate-descent for Volt/VAr control in distribution networks," *IEEE Trans. Power Syst.*, vol. 31, no. 6, pp. 4670–4678, Nov. 2016.
- [5] F. Olivier, P. Aristidou, D. Ernst, and T. Van Cutsem, "Active management of low-voltage networks for mitigating overvoltages due to photovoltaic units," *IEEE Trans. Smart Grid*, vol. 7, no. 2, pp. 926–936, Mar. 2016.
- [6] A. Keane, L. F. Ochoa, E. Vittal, C. J. Dent, and G. P. Harrison, "Enhanced utilization of voltage control resources with distributed generation," *IEEE Trans. Power Syst.*, vol. 26, no. 1, pp. 252–260, Feb. 2011.
- [7] P. Cuffe and A. Keane, "Voltage responsive distribution networks: Comparing autonomous and centralized solutions," *IEEE Trans. Power Syst.*, vol. 30, no. 5, pp. 2234–2242, Sep. 2015.
- [8] E. Dall'Anese, S. V. Dhople, and G. B. Giannakis, "Optimal dispatch of photovoltaic inverters in residential distribution systems," *IEEE Trans. Sustain. Energy*, vol. 5, no. 2, pp. 487–497, Apr. 2014.
- [9] M. Farivar, C. R. Clarke, S. H. Low, and K. M. Chandy, "Inverter VAR control for distribution systems with renewables," in *Proc. IEEE Int. Conf. Smart Grid Commun.*, Oct. 2011, pp. 457–462.
- [10] E. Dall'Anese, S. V. Dhople, B. B. Johnson, and G. B. Giannakis, "Decentralized optimal dispatch of photovoltaic inverters in residential distribution systems," *IEEE Trans. Energy Conv.*, vol. 29, no. 4, pp. 957–967, Dec. 2014.
- [11] P. Šulc, S. Backhaus, and M. Chertkov, "Optimal distributed control of reactive power via the alternating direction method of multipliers," *IEEE Trans. Energy Convers.*, vol. 29, no. 4, pp. 968–977, Dec. 2014.
- [12] M. Bazrafshan and N. Gatsis, "Decentralized stochastic optimal power flow in radial networks with distributed generation," *IEEE Trans. Smart Grid*, vol. 8, no. 2, pp. 787–801, Mar. 2017.

- [13] K. Turitsyn, P. Šulc, S. Backhaus, and M. Chertkov, "Options for control of reactive power by distributed photovoltaic generators," *Proc. IEEE*, vol. 99, no. 6, pp. 1063–1073, Jun. 2011.
- [14] M. Rylander, H. Li, J. Smith, and W. Sunderman, "Default volt-var inverter settings to improve distribution system performance," in *Proc. IEEE Power Energy Soc. Gen. Meeting*, Jul. 2016, pp. 1–5.
- [15] N. Li, G. Qu, and M. Dahleh, "Real-time decentralized voltage control in distribution networks," in *Proc. 52nd Annu. Allerton Conf. Commun., Control, Comput.*, Sep. 2014, pp. 582–588.
- [16] M. Farivar, X. Zhou, and L. Chen, "Local voltage control in distribution systems: An incremental control algorithm," in *Proc. IEEE Int. Conf. Smart Grid Commun.*, Nov. 2015, pp. 732–737.
- [17] K. S. Ayyagari, N. Gatsis, and A. F. Taha, "Chance constrained optimization of distributed energy resources via affine policies," in *Proc. IEEE Global Conf. Signal Inf. Process.*, Nov. 2017, pp. 1050–1054.
- [18] K. Baker, E. Dall'Anese, and T. Summers, "Distribution-agnostic stochastic optimal power flow for distribution grids," in *Proc. North Amer. Power Symp.*, Sep. 2016, pp. 1–6.
- [19] K. Baker, A. Bernstein, E. Dall'Anese, and C. Zhao, "Network-cognizant voltage droop control for distribution grids," *IEEE Trans. Power Syst.*, vol. 33, no. 2, pp. 2098–2108, Mar. 2018.
- [20] R. A. Jabr, "Linear decision rules for control of reactive power by distributed photovoltaic generators," *IEEE Trans. Power Syst.*, vol. 33, no. 2, pp. 2165–2174, Mar. 2018.
- [21] W. Lin and E. Bitar, "Decentralized stochastic control of distributed energy resources," *IEEE Trans. Power Syst.*, vol. 33, no. 1, pp. 888–900, Jan. 2018.
- [22] W. Lin, R. J. Thomas, and E. Bitar, "Real-time voltage regulation in distribution systems via decentralized PV inverter control," in *Proc. 51st Hawaii Int. Conf. Syst. Sci.*, 2018, pp. 2680–2689.
- [23] M. Lubin, Y. Dvorkin, and S. Backhaus, "A robust approach to chance constrained optimal power flow with renewable generation," *IEEE Trans. Power Syst.*, vol. 31, no. 5, pp. 3840–3849, Sep. 2016.
- [24] Y. Zhang, S. Shen, and J. L. Mathieu, "Distributionally robust chance-constrained optimal power flow with uncertain renewables and uncertain reserves provided by loads," *IEEE Trans. Power Syst.*, vol. 32, no. 2, pp. 1378–1388, Mar. 2017.
- [25] I. Roytelman and J. M. Palomo, "Volt/VAR control in distribution systems," 2016, pp. 195–225. [Online]. Available: http://digital-library.theiet.org/content/books/10.1049/pbpo075e_ch8
- [26] I. Džafić and R. A. Jabr, "Real time multiphase state estimation in weakly meshed distribution networks with distributed generation," *IEEE Trans. Power Syst.*, vol. 32, no. 6, pp. 4560–4569, Nov. 2017.
- [27] I. Roytelman, B. K. Wee, and R. L. Lugtu, "Volt/VAR control algorithm for modern distribution management system," *IEEE Trans. Power Syst.*, vol. 10, no. 3, pp. 1454–1460, Aug. 1995.
- [28] J. Carden and D. Popovic, "Closed-loop Volt/Var optimization: Addressing peak load reduction," *IEEE Power Energy Mag.*, vol. 16, no. 2, pp. 67–75, Mar. 2018.
- [29] V. Guigues, "Robust production management," *Optim. Eng.*, vol. 10, no. 4, pp. 505–532, 2009.
- [30] G. C. Calafiore and L. E. Ghaoui, "On distributionally robust chance-constrained linear programs," *J. Optim. Theory Appl.*, vol. 130, no. 1, pp. 1–22, Jul. 2006.
- [31] J. R. S. Mantovani, F. Casari, and R. A. Romero, "Reconfiguração de sistemas de distribuição radiais utilizando o critério de queda de tensão," *SBA, Controle Automaçã.*, vol. 11, no. 3, pp. 150–159, Dec. 2000.
- [32] "Robust VVC distribution network data and result sets." 2018. [Online]. Available: https://www.dropbox.com/s/fx7yolxjvc3hy9/Robust_VVC_Net.zip?dl=0. Accessed on: Oct. 30, 2018.
- [33] "IBM ILOG CPLEX. ver. 12.7." 2016. [Online]. Available: <https://www.ibm.com/products/ilog-cplex-optimization-studio>
- [34] EPRI, "Common functions for smart inverters," 4th ed., EPRI, Palo Alto, CA, USA, Rep. 3002008217, 2016.



Rabih A. Jabr (M'02–SM'09–F'16) was born in Lebanon. He received the B.E. degree in electrical engineering (with high distinction) from the American University of Beirut, Beirut, Lebanon, in 1997, and the Ph.D. degree in electrical engineering from the Imperial College London, London, U.K., in 2000. He is currently a Professor with the Department of Electrical and Computer Engineering, American University of Beirut. His research interests are in mathematical optimization techniques and power system analysis and computing.